



Jurnal Teknologi Reaktor Nuklir

Tri Dasa Mega

Journal homepage: jurnal.batan.go.id/index.php/tridam

Collision Cascade and Primary Radiation Damage in Silicon Carbide: A Molecular Dynamics Study

Ihda Husnayani^{1*}, Muzakkiy Putra Muhammad Akhir²¹Research Center for Nuclear Reactor Technology, National Research and Innovation Agency, Kawasan Puspitek Gedung 80, Tangerang Selatan, Banten, Indonesia²Research Center for Quantum Physics, National Research and Innovation Agency, Kawasan Puspitek Gedung 440, Tangerang Selatan, Banten, Indonesia

ARTICLE INFO

Article history:

Received: 21 September 2022

Received in revised form: 17 October 2022

Accepted: 17 October 2022

Keywords:

Silicon carbide
Collision cascade
Radiation damage
Molecular dynamics
Neutron irradiation

ABSTRACT

Silicon carbide (SiC) is a competitive candidate material to be used in several advanced and Generation-IV nuclear reactor designs as a neutron moderator, fuel coating, cladding, or core structural material. Many studies have been performed to investigate the durability of SiC in a severe environment in a nuclear reactor. However, the nature and behavior of defects induced by neutron irradiation are still not fully understood. This paper is aimed to study collision cascade and primary radiation damage in SiC using molecular dynamics simulation. The potential being used was a hybrid Tersoff potential modified with Ziegler-Biersack-Littmark (ZBL) screening function. The collision cascade was let evolved for 10 ps from a Si or C primary knocked atom (PKA) located initially at the top center of a system containing 960.000 atoms. The simulation was carried out at room temperature as well as at several advanced fission reactor-relevant temperatures. It was obtained that the number of C point defects was larger than the number of Si point defects. The number of stable point defect was found to be temperature-dependent. It was also obtained that the recovery of point defects was larger at high temperature (>800°C). This recovery behavior shows that SiC is suitable to be used at high temperature condition.

© 2022 Tri Dasa Mega. All rights reserved.

1. INTRODUCTION

Silicon carbide (SiC), although it has been used in nuclear reactor application since 60 years ago as a coating material of High Temperature Gas-cooled Reactor (HTGR) fuel, is still a competitive material to be used in advanced reactor designs currently being developed [1–3]. Besides its use in HTGR, SiC coated fuel particles are also used in pebble-bed molten salt reactor (PB-MSR) design [4]. SiC is also

a strong candidate material for accident tolerant fuel (ATF) cladding in light water reactor-based small modular reactor (SMR) [5, 6]. Moreover, SiC is currently proposed to be used as coating for graphite in MSR to protect graphite from salt infiltration [7, 8]. The properties of SiC which make it desirable for use in nuclear reactors are its excellent mechanical strength in high-temperature, radiation and oxidation resistance. However, it is known that properties modification of SiC might occur due to neutron

*Corresponding author

E-mail: ihda001@brin.go.id

DOI: 10.17146/tdm.2022.24.3.6702

irradiation at different irradiation environment, such as different fluence and temperature. Currently, study about radiation damage on SiC is still massively being performed.

Besides the studies of radiation damage performed through irradiation experiment such as reported in Ref. [9–11], it can also be performed through computational means. One of many types of computational study ubiquitously used to study radiation damage in atomic scale is Molecular Dynamics (MD) simulation. From MD simulation, the mechanism of radiation damage production can be understood from early stage. When a particle or radiation, for example a neutron, hits the first atom in SiC, it will displace the atom (Primary Knock-on Atom/PKA) from its original position. This atom then hit another atom in the lattice and so on until it forms a phenomenon called collision cascade. At the end of the collision cascade, primary damage in terms of Frenkel pair (vacancy and interstitial) might occur. Several recent studies regarding radiation damage in SiC include the effect of electronic stopping on collision cascade of SiC [12, 13], defect cluster distribution in ion irradiated SiC [14], and comparison of interatomic potential for cascade simulation of SiC [15].

In this work, the collision cascade and primary damage production on SiC induced by neutron irradiation was studied using MD simulation. The simulations were performed at several temperature values which correspond to the temperature of several advanced nuclear reactor designs [300°C (APWR), 550°C (SFR, LFR, SCWR), 800°C (MSR, GFR), and 1000°C (VHTR)] [16]. The cubic structure of SiC (3C-SiC) was used in the simulation since it is the most common type of SiC used in nuclear reactor applications. The primary damages analyzed were the number of vacancies and interstitials, also in terms of replacement and antisites. These damages are the common types of primary radiation damage found in ceramic material.

2. THEORY

A classical MD simulation is a computer simulation method to track the movement of atoms or molecules based on Newton's equation of motion. The basic flow in MD simulation is at first having a system consisting a set of atoms with known mass m , initial position \mathbf{r}^i , and velocity \mathbf{v}^i . A potential V describing the interaction between those atoms is set. Then the force \mathbf{F} acting between the atoms is calculated which is the gradient of potential [17],

$$\mathbf{F} = -\nabla V(\mathbf{r}) \quad (1)$$

The acceleration \mathbf{a} can be determined using Newton's law,

$$\mathbf{a} = \mathbf{F}/m \quad (2)$$

Since the atoms will move based on the potential and acceleration, after a specific timestep Δt , the position and velocity of each atom can be updated,

$$\mathbf{r}^{i+1} = \mathbf{r}^i + \mathbf{v}^i \Delta t + \frac{1}{2} \mathbf{a} \Delta t^2 \quad (3)$$

$$\mathbf{v}^{i+1} = \mathbf{v}^i + \mathbf{a} \Delta t \quad (4)$$

The timestep can then move forward to the next timestep $t = t + \Delta t$ and the updated position and velocity then become the initial position and velocity. The force and acceleration then recalculated and the position and velocity are also reupdated. This cycle can be repeated as many as intended.

The position and velocity of each atoms at each time steps can be used for calculating observables and thermodynamic properties of the system. All of those calculations are performed numerically using specific numerical integrator and algorithm such as Verlet Algorithm, Beemans Algorithm, etc.

The MD simulation can be performed using specific thermodynamics ensemble depending on the simulated system and the targeted thermodynamical properties. Those ensembles are microcanonical, canonical, and isothermal-isobaric ensemble. Interatomic potential or force field used to describe the interaction between atoms or molecules can be an empirical potential, semi-empirical potential, or ab-initio potential. Further detail regarding molecular dynamics simulation can be found in many textbooks, one of which is "Understanding Molecular Simulation: From Algorithms to Applications," a book by Berend Smit and Daan Frenkel.

3. METHODOLOGY

In this study, the MD simulation was performed using an open source classical MD software developed by Sandia National Laboratory named Large-scale Atomic/Molecular Massively Parallel Simulator (LAMMPS) [18]. The crystal structure of 3C-SiC is cubic zincblende structure with lattice parameter of 4.359 Å. The simulation box was created using 40×40×75 unit cells (~960.000 atoms). Periodic boundary condition was used in all directions. To avoid any unphysical effects during the simulation, five outermost layers excluding the top layers were set as thermostat. Temperature of the thermostat was maintained at the simulation temperature using velocity rescaling. The simulations were performed for five temperature variations; one is room temperature and the other four are the temperature of several advanced fission reactors [300° C (APWR), 550° C (SFR, LFR, SCWR), 800° C (MSR, GFR), and 1000° C (VHTR)] [16].

Tersoff/ZBL was chosen as the interatomic potential for 3C-SiC. This is a three-body hybrid potential with a close-separation pairwise modification based on a Coulomb potential and the Ziegler-Biersack-Littmark universal screening function [19]. This potential had been checked before performing the simulation and it was able to produce the lattice constant and cohesive energy. The collision cascade in the simulation box was initiated by Primary Knock-on Atom (PKA) having energy of 10 keV in $[4\ 11\ \bar{9}5]$ direction. High index direction was chosen to avoid or minimize the channeling effect. Two types of simulations were performed, namely single silicon PKA and single carbon PKA. The PKA was defined at the top center of simulation box.

The system was equilibrated first for 1 ps using NVE microcanonical ensemble along with temperature rescaling of the thermostat. Second equilibration was performed for another 1 ps but without temperature rescaling of the thermostat. With this, energy was allowed to leave the system through interaction with thermostat region, but the thermostat does not affect the energy in the simulation domain. The observation of collision cascade in three phases (initial, intermediate, final phases). The initial phase with 0.01 fs timestep was run for 0.1 ps, the intermediate phase with 0.1 fs timestep was run for 1 ps, and the final phase with 1 fs timestep was run for 10 ps.

Defects identification and counting was performed using voronoi diagram analysis in terms of total vacancy and interstitial, C and Si vacancy, C and Si replacement, C_{Si} and Si_C antisite. The first step of the initial phase was used as reference geometry and as the center for 3D Voronoi diagram. The type of defect was identified based on the cell's occupancy. If the cell's occupancy is less than 1, it means a vacancy. If the cell's occupancy is more than 1, it means an interstitial. If a previously empty cell (vacancy) is then filled with the same atom it is called a replacement, while if it is filled with different atom it is called an antisite.

4. RESULTS AND DISCUSSION

Fig. 1 shows the visualization of the collision cascade event of one Si PKA at several timesteps. Blue atoms are silicon and red ones are carbon. Atoms with coordination number 4 were deleted so only atoms affected by the collision cascade were visualized. It can be seen that the collision cascade gradually escalated and reached maximum at around 1 ps. The number of affected atoms was also maximum at this timestep. This is when all kinetic energy owned by the PKA had been fully transferred

during the cascade. After that, the number of affected atoms decreased until saturation was reached. It can be deduced from the figure that the concentration of affected atoms are saturated after 1 ps. This is clearly due to the recombination event of Frankel pairs.

Fig. 2 and Fig. 3 show the graph containing plot of the number of point defect count versus timestep. Several things can be inferred from the figure. The total vacancy (and also total interstitial because of the Frankel pair) started emerging at 0.01 ps and gradually increased until reached maximum at around 1.2 ps, then it gradually decreased until reached steady-state and became the surviving "stable" point defects. Quotation marks are used to emphasize that it is stable in this particular time frame. The number of carbon vacancy (C-vac) is always higher than silicon vacancy (Si-vac) by a factor of 3-5. This is due to the lower threshold displacement energy of carbon atom than one of silicon, so that carbon are easier to move [19].

In all cases, the number of carbon self-replacement (C-rep) is always higher than silicon self-replacement (Si-rep) and the number of Si_C antisite (Si_C-ant, silicon replacing vacant carbon site) is always higher than C_{Si} antisite (C_{Si}-ant, carbon replacing vacant silicon site). However, although C-rep and Si_C-ant which are responsible for the recovery of C-vac are always higher, the recovery rate of C-vac is always lower than one of Si-vac. This is because C-vac emerges more rapidly during the cascade so that the net recovery of C-vac is lower than one of Si-vac.

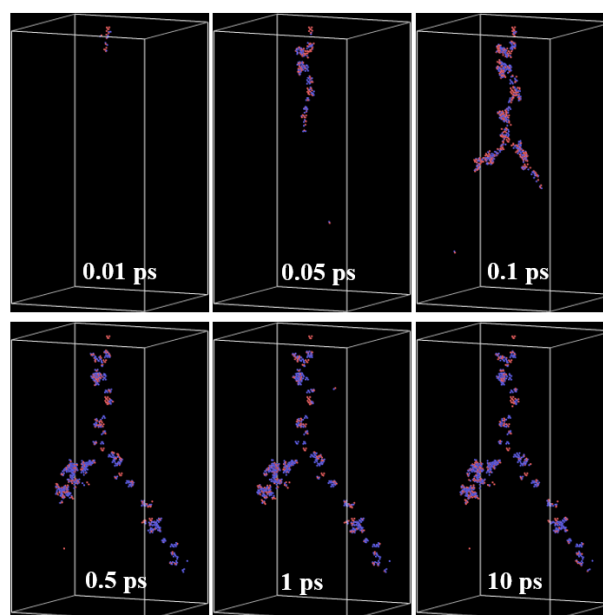


Fig. 1. Snapshot of collision cascade process at several timesteps (one Si PKA at 823 K)

At different simulated temperatures (RT, 573, 823, 1073, and 1273 K) which corresponds to different nuclear reactor working temperatures [300° C (APWR), 550° C (SFR, LFR, SCWR), 800° C (MSR, GFR), and 1000° C (VHTR)] and can further correspond to the different annealing temperatures, no major difference in the trend of the graph (Fig. 2 and Fig 3) has been found which means that the behavior of point defects at those temperature is almost the same.

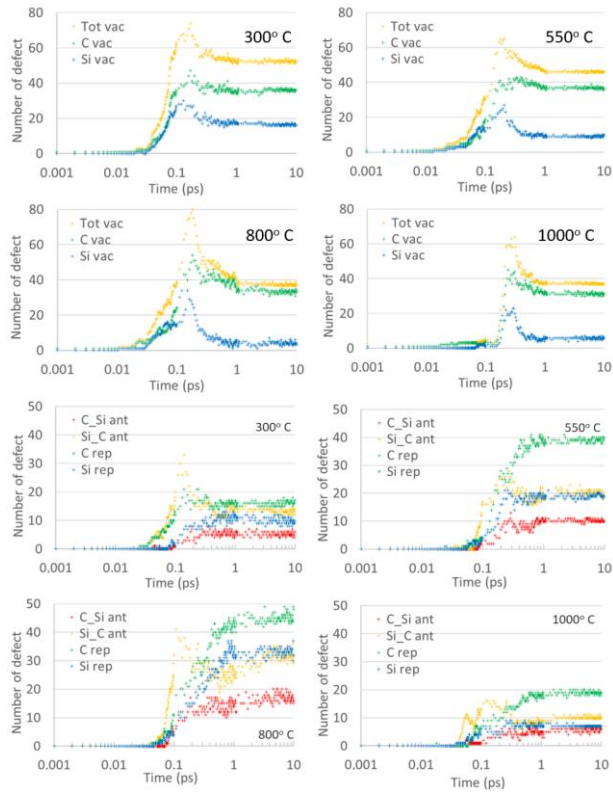


Fig. 2. Plot of the number point defects versus simulation time for single silicon PKA

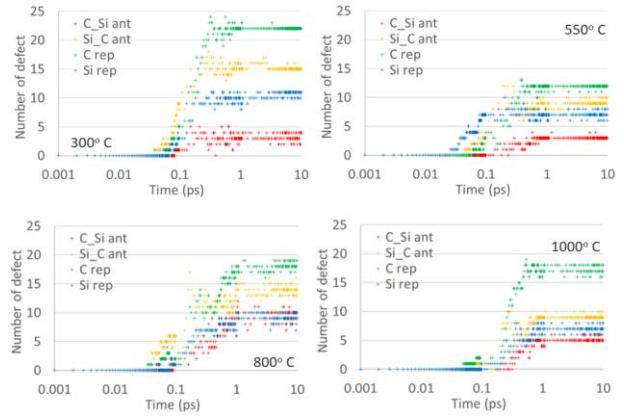
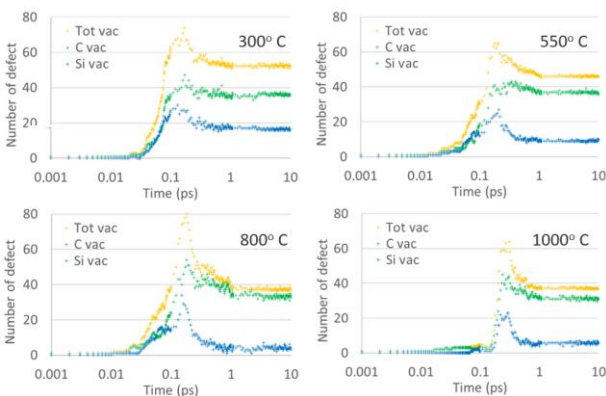


Fig. 3. Plot of the number point defects versus simulation time for single carbon PKA

However, the number of stable Frankel pairs at the end of simulation (10 ps) is different at different temperatures as shown in Fig. 4. It emphasizes that the number of stable point defect tend to be maximum at around 823K (500°C) and then decreases at higher temperature.

After reaching maximum value, the Frankel pairs decreases until it reaches steady state within 0.7-0.8 ps. The antisites, on the other hand, appears to be more stable than the Frankel pairs. A slight reduction of Si_C-ant is seen in several cases which possibly due to the instability of this defect near Si vacancy.

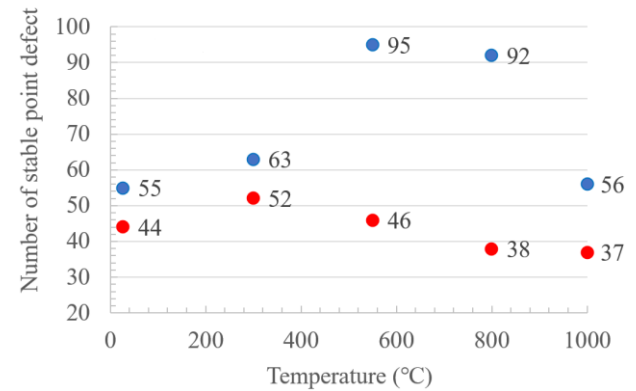


Fig. 4. Plot of the number of stable point defects versus temperature (blue circles are for silicon PKA, red circles are for carbon PKA)

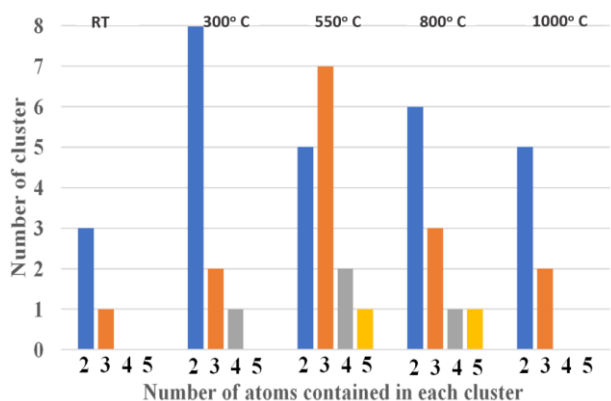


Fig. 5. Results of cluster identification at different temperature (for single Si PKA)

Cluster identification with nearest neighbor analysis using cut off distance of 2.2 Å, which is slightly larger than 1.9 Å nearest neighbor spacing but smaller than the second neighbor spacing, show that the number of interstitial clusters reached maximum also at 823K and then decreased at higher temperature (Fig. 5). It was found that the most concentrated distribution of stable point defects was found at 823K. The biggest cluster contains 5 interstitials. This indicates that temperature below 823K is the point defect regime and around 823K is the cluster regime. Above 823K, although the simulation suggests back to point defect regime, it should be the regime for the more complex higher dimensional defect because the measured thermal conductivity was not recovered. This again builds up the conclusion of different stable form of defect and different underlying recovery mechanism at different temperature.

5. CONCLUSION

The collision cascade and primary radiation damage was studied using molecular dynamics simulation. The simulations were performed for single Si PKA and single C PKA at room temperature and several advanced fission reactor temperatures. It was obtained that the number of total point defect, from either Si PKA or C PKA, was found to be maximum at around 0.1ps before it gradually decreased to a stable amount. It was also found that the number of C point defect was always larger than one of the Si and the recombination of Si vacancies tended to be larger than the recombination of C vacancies. The number of stable point defect was found to be increasing as the temperature increased, but then started decreasing at around 800°C, indicating that the recovery of point defect is larger at higher temperatures. Aside from the dependency to temperature, the energy of PKA might also affects the collision cascade events and

the production of primary radiation damage. Investigation of collision cascade and primary radiation damage at various energies dan number of PKAs can be a good topic for further study.

AUTHOR CONTRIBUTION

Ihda Husnayani and Muzakkiy Putra M. A. equally contributed as the main contributors of this paper. All authors read and approved the final version of the paper.

REFERENCES

1. Katoh Y., Snead L.L. Silicon Carbide and Its Composites for Nuclear Applications – Historical overview. *J. Nucl. Mater.* 2019. **526**:151849.
2. Taryo T., Husnayani I., Subekti R.M., Sudadiyo S., Saragi E., Rokhmadi The Development of HTGR-TRISO Coated Fuels in the Globe: Challenging of Indonesia to be an HTGR Fuel Producer. *J. Phys. Conf. Ser.* 2019. **1198**(2).
3. Demkowicz P.A., Liu B., Hunn J.D. Coated Particle Puel: Historical Perspectives and Current Progress. *J. Nucl. Mater.* 2019. **515**:434–50.
4. Lee J.J., Raiman S.S., Katoh Y., Koyanagi T., Contescu C.I., Hu X., et al. Chemical Compatibility of Cilicon Carbide in Molten Fluoride Salts for the Fluoride Salt-cooled High Temperature Reactor. *J. Nucl. Mater.* 2019. **524**:119–34.
5. Qiu C., Liu R., Cai J., Zhou W. Multiphysics Analysis of Thorium-based Fuel Performance with a Two-layer SiC Cladding under Normal Operating and Transient Conditions in a Light Water Reactor. *Ann. Nucl. Energy.* 2021. **163**:108543.
6. Liang Y., Lan B., Zhang Q., Seidl M., Wang X. Neutronic Analysis of Silicon Carbide Cladding-ATF Fuel Combinations in Small Modular Reactors. *Ann. Nucl. Energy.* 2022. **173**:109120.
7. Lee J.J., Arregui-Mena J.D., Contescu C.I., Burchell T.D., Katoh Y., Loyalka S.K. Protection of Graphite from Salt and Gas Permeation in Molten Salt Reactors. *J. Nucl. Mater.* 2020. **534**
8. He Z., Song J., Lian P., Zhang D., Liu Z. Excluding Molten Fluoride Salt from Nuclear Graphite by SiC/glassy Carbon Composite Coating. *Nucl. Eng. Technol.* 2019. **51**(5):1390–7.
9. Sreelakshmi N., Amirthapandian S., Umopathy G.R., David C., Srivastava S.K., Ojha S., et al. Raman Scattering Investigations on Disorder

- and Recovery Induced by Low and High Energy Ion Irradiation on 3C-SiC. *Mater. Sci. Eng. B Solid-State Mater. Adv. Technol.* 2021. **273**(March):115452.
10. Mirzayev M.N., Abdurakhimov B.A., Demir E., Donkov A.A., Popov E., Tashmetov M.Y., et al. Investigation of the Formation of Defects under Fast Neutrons and Gamma Irradiation in 3C-SiC nano powder. *Phys. B Condens. Matter.* 2021. **611**(January):412842.
 11. Lach T.G., Le Coq A.G., Linton K.D., Terrani K.A., Byun T.S. Characterization of Radiation Damage in 3D Printed SiC. *J. Nucl. Mater.* 2022. **559**:153459.
 12. Wu J., Xu Z., Zhao J., Rommel M., Nordlund K., Ren F., et al. MD Simulation of Two-Temperature Model in Ion Irradiation of 3C-SiC: Effects of Electronic and Nuclear Stopping Coupling, Ion Energy and Crystal Orientation. *J. Nucl. Mater.* 2021. **557**:153313.
 13. Zarkadoula E., Samolyuk G., Zhang Y., Weber W.J. Electronic Stopping in Molecular Dynamics Simulations of Cascades in 3C-SiC. *J. Nucl. Mater.* 2020. **540**:152371.
 14. Liu C., Szlufarska I. Distribution of Defect Clusters in the Primary Damage of Ion Irradiated 3C-SiC. *J. Nucl. Mater.* 2018. **509**:392–400.
 15. Samolyuk G.D., Osetsky Y.N., Stoller R.E. Molecular Dynamics Modeling of Atomic Displacement Cascades in 3C-SiC: Comparison of Interatomic Potentials. *J. Nucl. Mater.* 2015. **465**:83–8.
 16. Zinkle S.J., Was G.S. Materials Challenges in Nuclear Energy. *Acta Mater.* 2013. **61**(3):735–58.
 17. Arkundato A., Su'Ud Z., Abdullah M., Sutrisno W., Celino M. Inhibition of Iron Corrosion in High Temperature Stagnant Liquid Lead: A Molecular Dynamics Study. *Ann. Nucl. Energy.* 2013. **62**:298–306.
 18. Thompson A.P., Aktulga H.M., Berger R., Bolintineanu D.S., Brown W.M., Crozier P.S., et al. LAMMPS - a Flexible Simulation Tool for Particle-based Materials Modeling at the Atomic, Meso, and Continuum Scales. *Comput. Phys. Commun.* 2022. **271**:108171.
 19. Devanathan R., Diaz De La Rubia T., Weber W.J. Displacement Threshold Energies in β -SiC: Section 2. Radiation Effects in Monolithic SiC-based Ceramics. *J. Nucl. Mater.* 1998. **253**(1–3):47–52.